Spin-Polarized Nitroxide Radicals in Organic Glasses†

Valery F. Tarasov,* Ilya A. Shkrob, and Alexander D. Trifunac*

Chemistry Division, Argonne National Laboratory, Argonne, Illinois 60439

Received: December 5, 2001; In Final Form: March 4, 2002

Nonequilibrium spin polarization formed in a stable nitroxide radical, 2,2,6,6-tetramethyl-1-piperidinyloxy (Tempo) due to the occurrence of Chemically Induced Dynamic Electron Polarization (CIDEP) in photoexcited molecular complexes of this radical with 1,4-benzoquinone, 1,4-naphthaquinone, 9,10-anthraquinone, and their derivatives is observed. These complexes occur spontaneously in low-temperature organic glasses (20−70 K) upon freezing the concentrated liquid solutions. The emissive net polarization in the nitroxide radical is observed 0.1−10 μs after the photoexcitation of the *p*-quinone moiety. No degradation of the polarized magnetic resonance signal from Tempo after $>10^4$ excitation cycles was observed. This spin polarization is shown to be mainly due to a polarization transfer from the lowest triplet state of the *p*-quinone. This transfer is driven by the electron spin exchange interaction between the nitroxide radical and the triplet *p*-quinone; it occurs simultaneously with a spin-selective electronic relaxation of the photoexcited complex. The resulting mechanism combines the features of the electron spin polarization transfer (ESPT) and radical−triplet pair mechanisms (RTPM) in liquid. A theoretical model of such a mechanism is suggested.

1. Introduction

Stable nitroxide radicals, such as 2,2,6,6-tetramethyl-1-piperidinyloxy (Tempo), are known to quench the lowest triplet (T_1) states of aromatic molecules in liquid solutions. [1] Magnetic interactions between these triplets and the nitroxide radicals result in the formation of nonequilibrium electron spin polarization in the latter.[2−5] Before this nonequilibrium polarization decays by spin−lattice relaxation, it can be observed using time-resolved electron paramagnetic resonance (TR EPR) spectroscopy.[2−5]

Two mechanisms for the electron spin polarization in the radical−triplet encounters in a liquid solution have been suggested. One mechanism is the electron spin polarization transfer (ESPT)[3] and another is the radical triplet pair mechanism (RTPM).[4−7] In ESPT, nonequilibrium spin polarization of the T_1 state (due to state-selective intersystem crossing) is "transferred" to the radical. To our knowledge, no specific details for this mechanism have been suggested.

In RTPM, the initial spin polarization in the T_1 state is not required. The exchange interaction between the triplet (spin-1) and the nitroxide radical (spin-$^1/_2$) splits the spin states of the encounter complex into the doublet (spin-$^1/_2$) and the quartet (spin-$^3/_2$) excited states.[4−6] While the spin-$^1/_2$ states of the encounter complex rapidly relax to the ground state of this complex (in which the partner of the radical is in the lowest S_0 state), the spin-$^3/_2$ states of the encounter complex are dissociative. The interplay between this spin-selective reaction and the distance-dependent exchange interaction results in the electron spin polarization in the radical. A detailed theory of RTPM has been suggested by Adrian,[7] Shushin,[6] and Kobori et al.[8] The RTPM polarization depends on the lifetime of the encounter complex and the rotation correlation time of the triplet (both of which are controlled by the solvent viscosity), the dipole interaction in the triplet, and the spin exchange potential.[4,5]

In liquid, rotational and translational diffusion complicates the theoretical treatment of the spin dynamics. Various simplifying assumptions concerning the molecular dynamics, kinetics, and energetics of the encounter complex have to be made,[6,7,8] with little experimental support. When the rotational/translational motion is eliminated, the spin dynamics becomes more tractable. Recently, several photosystems in which the nitroxide radical is chemically bound to an organic moiety (for example, a phthalocyaninesilicon,[9] porphyrin,[10] or a fullerene[11] molecule) have been studied by X and W band TR EPR. Spin dynamics observed in these photosystems were interpreted in terms of the RTPM: however, no detailed mechanistic studies were carried out.

In the present work, spin polarization mechanisms that are peculiar to radical−triplet complexes immobilized in frozen organic glasses are examined. We found that neither the "polarization transfer" (as in ESPT) nor the spin-selective reaction (as in RTPM) alone are capable of reproducing the spin polarization observed in such molecular complexes. We are not aware of other low-temperature studies of spin polarization caused by the radical−triplet interaction in a molecular solid except for the work in ref 12.

A possible application for the matrix-isolated spin-polarized radicals is quantum computing.[13−17] This technology requires efficient ways to generate highly coherent, entangled quantum states characterized by long decoherence and disentanglement times.[13,14] Electron and nuclear spins are particularly convenient due to their relative isolation from other degrees of freedom.[13] In a quantum computer, the spins (qubits) should weakly interact with each other[15,16,17] and be addressable individually ("spin communication"). Prototype devices based on the manipulation of coupled nuclear spins in an organic molecule have been reported.[15] While these NMR devices prove several important concepts, the NMR approach cannot be scaled to the thousands of qubits that are needed to solve practically important

† Work performed under the auspices of the Office of Basic Energy Sciences, Division of Chemical Science, US-DOE under contract number W-31-109-ENG-38.

* To whom the correspondence should be addressed.

10.1021/jp014406p CCC: $22.00
Published on Web 04/18/2002

problems.[13] An alternative has been proposed[13,16,17] to use lithographically patterned semiconductor devices containing strategically placed impurity[16] and/or artificial[17] atoms. A hybrid device, in which stable organic radicals are anchored on the semiconductor surface could be more practicable. Our work is the first step toward such a hybrid device.

2. Experimental

The compounds 9,10-anthraquinone, 1,4-naphthoquinone, and 1,4-benzoquinone (Aldrich) were twice recrystallized from ethanol. All other chemicals were of the highest purity grade and used as received from Aldrich. The concentration of aromatic photosensitizers was 1−10 mM; the concentration of Tempo was 10−100 mM (the exact concentrations are given in the figure captions). The oxygen was removed by several freeze−pump−thaw cycles; control experiments showed that oxygen had no effect on the TR EPR spectra. Liquid solutions were placed in 4 mm o.d. suprasil tubes, deoxygenated, sealed, and freeze-quenched by immersion in liquid nitrogen. These frozen samples were placed in an Oxford Instruments CF 935 cryostat and irradiated in situ. No difference between the TR EPR of the samples obtained using different cooling/freezing procedures was found. No TR EPR signals in the laser photolysis of Tempo solutions without the photosensitizers (*p*-quinones) were observed.

A Quantel Brilliant Nd:YAG laser was operated at 355 nm (third harmonic, 6 ns fwhm) with a pulse energy of 10−20 mJ. TR EPR experiments were performed using a Bruker ER047 XG-T bridge that was operated at 10 mW in the X band. The EPR signal from a 12 MHz preamplifier of this microwave bridge was sampled using either an SRI 245 boxcar integrator-averager (with the gate width of 250 ns) or a Tektronix TDS 420A digital oscilloscope. The delay times given below were not corrected for the response time of the detection system. The *Q* factor of the EPR cavity was less then 800. Therefore, the time resolution of device was limited by the bandwidth of preamplifier. The first derivative cw EPR spectra of Tempo solutions were obtained using a modulation field of 0.02 mT, a modulation frequency of 100 kHz, and a microwave power of 1−10 mW.

3. Results

Figures 1−3 show the TR EPR spectra obtained in the laser photolysis of 1,4-benzoquinone, 2,6-dimethyl-1,4-benzoquinone, and 2,3,5,6-tetramethyl-1,4-benzo-quinone (Figure 1); 1,4-naphthoquinone, 2-methyl-1,4-naphthoquinone, and 2,3-dichloro-1,4-naphthoquinone (Figure 2); and 9,10-anthraquinone and 2-methyl-9,10-anthraquinone (Figure 3) in a toluene glass containing 10−100 mM Tempo at 60 K. The upper traces show the TR EPR spectra from the emissively polarized Tempo. In the lower traces (obtained using a wider magnetic field sweep) the narrow EPR signals from Tempo are indicated by asterisks; broad, emissive/absorptive EPR signals extending over 1 T are from spin-polarized T_1 states of the *p*-quinones. The spectra shown in Figures 1−3 were obtained 0.5 μs after a 6 ns fwhm, 10 mJ, 355 nm laser pulse. The following general trends were observed.

Among several aromatic photosensitizers examined in this work (such as benzophenone, benzil, naphthalene, nitro-naphthalene, anthracene, and porphyrins), only *p*-quinones produced spin polarization in the nitroxide radical. Not every quinone was effective: photoexcitation of duroquinone, 2,3,5,6-tetrafluoro-1,4-benzo-quinone, and *o*-naphthoquinone did not yield spin polarized radicals. Spin-polarized Tempo was observed only in frozen hydrocarbons, such as toluene and methylcyclohexane. In ethanol glass, TR EPR spectra of the *p*-quinone triplets were readily observable. However, no polarized nitroxide radicals were observed in this glass, nor were such radicals observed in toluene and methylcyclohexane glasses that contained more than 20 vol % of the alcohol.

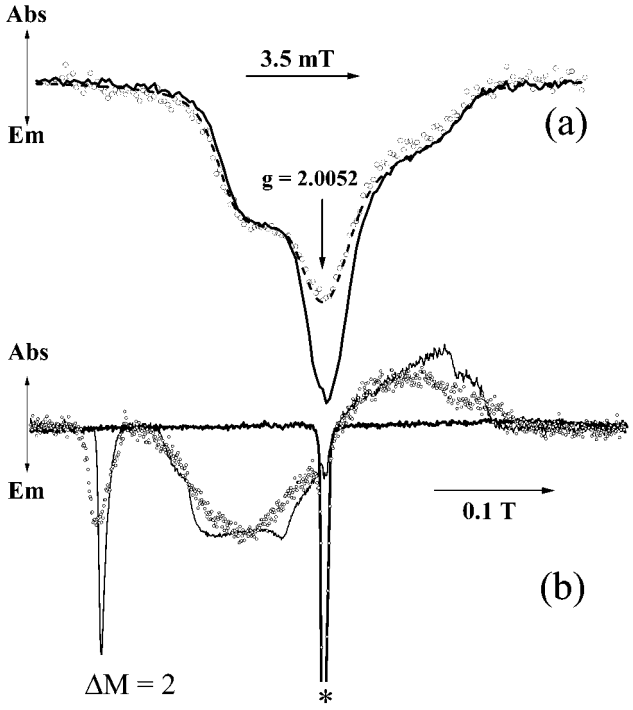

Figure 1. Time-resolved X band EPR spectra obtained in the 355 nm laser photolysis of Tempo/*p*-quinone solutions in frozen toluene glass at 60 K (see sections 2 and 3 for more detail). Traces (a) (narrow field sweep; normalized) and (b) (wide sweep; not normalized) were obtained under the same experimental conditions at the delay time 0.5 μs and the boxcar gate of 0.25 μs. The photosystems were 86 mM Tempo and 3.8 mM 1,4-benzoquinone (bold solid line), 76 mM Tempo and 5.9 mM 2,6-dimethyl-1,4-benzoquinone (open circles), 79 mM Tempo and 6.1 mM 2,3,5,6-tetramethyl-1,4-benzoquinone (thin solid line). A normalized inverted first-derivative EPR spectrum of Tempo from the same 1,4-benzoquinone solution before laser irradiation is shown by a bold dashed line in traces a. In traces b, the emissive signal at the center indicated by an asterisk is from spin-polarized Tempo (shown in more detail in traces a); the wide emissive/absorptive signals are from the $\Delta M = \pm 1$ transitions in the *p*-quinone triplets. The low-field emissive signal in traces b is from the $\Delta M = 2$ transition in these triplets.

The substrate/solvent specificity suggests that Tempo is polarized due to photoexcitation of *a preexisting molecular complex* of the nitroxide radical and a *p*-quinone. The formation of such a complex is supported by strong thermochromism observed in methylcyclohexane solutions of Tempo containing 2,3,5,6-tetrafluoro-1,4 benzoquinone or *o*-naphthoquinone. Interestingly, the quinone/Tempo solutions that showed strongest thermochromism did not yield spin polarization in the nitroxide radical. Apparently, the orbital mixing between the nitroxide radical and the *p*-quinone must be weak; otherwise, no spin polarization can be formed. That the molecular complexes do not form in polar solvents also suggests that the binding is weak. In nonpolar solvents, the complexation equilibrium is shifted toward a free *p*-quinone molecule and a nitroxide radical. In the room-temperature toluene solutions, the UV spectra of the *p*-quinones do not change upon the addition of Tempo, and the cw EPR spectra of Tempo do not change upon the addition of the *p*-quinones. High concentration of Tempo (0.02−0.1 M)

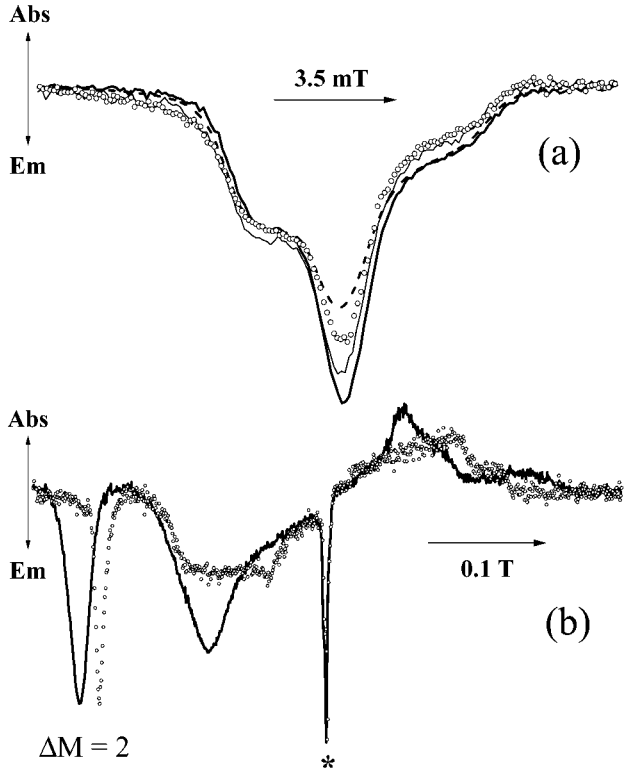

Figure 2. See the legend to Figure 1. The photosystems are 66 mM Tempo with 5.7 mM 1,4-naphthoquinone (bold line), 79 mM Tempo with 5.7 mM 2-methyl-1,4-naphthoquinone (thin solid line; not shown in (b)), and 89 mM Tempo and 2.3 mM 2,3-dichloro-1,4-naphthoquinone (open circles).

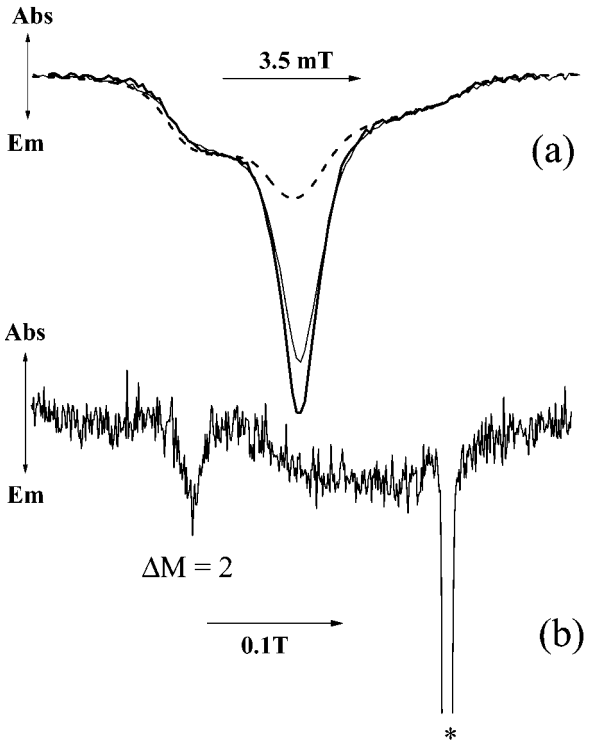

Figure 3. See the legend to Figure 1. The photosystems are 58 mM Tempo and 1.9 mM 1,9-anthraquinone (bold solid line) and 56 mM Tempo and 2.5 mM 2-methyl-1,4-anthraquinone (thin solid line). Only the TR EPR spectrum from 2-methyl-1,4-anthraquinone is shown in trace b.

must be used in order to shift the equilibrium and obtain the sufficient concentration of the molecular complexes.

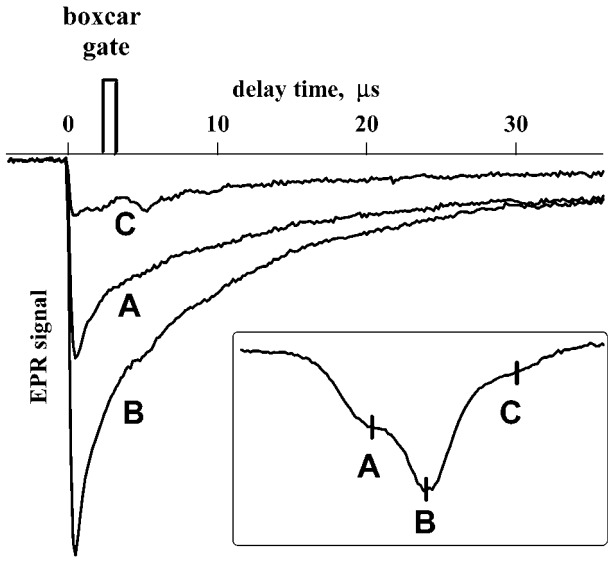

Figure 4. TR EPR signal from the spin polarized Tempo as function of the delay time after the 355 nm laser pulse. The photosystem is 3.5 mM 2,3-dichloro-1,4-naphthoquinone and 72 mM TEMPO in toluene glass at 60 K. The insert below shows the emissive TR EPR spectrum acquired by integration of the kinetics in the 2.4−3 μs window. The tics indicate the resonance magnetic fields where the kinetic traces A, B, and C were obtained.

Though the line shape of the TR EPR signal from the quinone triplet does not change in the presence of Tempo, the absolute signal rapidly decreases when the concentration of Tempo increases. This behavior suggests that wide EPR signals are from *free* quinone triplets that are not bound to the nitroxide radicals. The EPR signals of the bound triplets (or the quartet states of the complex) have not been observed. This could well be due to fast relaxation of bound triplet and inadequate time resolution of our TR EPR spectrometer to detect the nonrelaxed bound triplet and inadequate sensitivity to detect the relaxed one. The later is true even for free quinone triplets.

The line shapes of the TR EPR spectra obtained in the photolysis of glassy *p*-quinone/Tempo/toluene solutions and the integrated first derivative EPR spectra of Tempo obtained prior to the photoexcitation are compared in Figures 1a, 2a, and 3a. In the first 500 ns after the laser pulse, the line shape of the TR EPR spectrum is different from that of the thermalized radical: the central component of the spectrum (marked B in Figure 4) is *relatively* stronger than the spectral wings (marked A and C in Figure 4). This feature is most clearly seen in the TR EPR spectrum for 9,10-anthraquinone (Figure 3) and, to a lesser degree, in the TR EPR spectrum for 1,4-naphthoquinone (Figure 2). Only for 2,6-dimethyl-1,4- benzoquinone did the EPR line shape of the polarized signal match the EPR line shape of the thermalized signal perfectly (Figure 1). It is unclear, whether the short-lived "central component" is from Tempo or another radical (and/or radical ion) formed in a side photoreaction. There were no detectable TR EPR signals due to a laser-induced photoreaction of 1,4-benzoquinone with the toluene matrix (without Tempo); for 9,10-anthraquinone, only a very weak emissively polarized TR EPR signal was found. Therefore, the photoreaction that yields the "central component" involves Tempo.

In frozen methylcyclohexane solutions of 9,10-anthraquinone and 1,4-naphthaquinone, the TR EPR signal from Tempo overlaps with a weaker signal from a carbon-centered radical (perhaps formed in a hydrogen abstraction reaction of a T_n state with the solvent). Similar photoreaction may also occur in

toluene. It may account for a weak (ca. 15% of the polarized EPR signal from Tempo), slowly decaying emissive TR EPR signal that is observed at very long delay times (>20 μs). This weak, long-lived signal is not related to the "central component" observed on the submicrosecond time scale.

Figure 4 exhibits typical TR EPR kinetics observed for the $M[^{14}N] = -1$, 0, and +1 resonance lines in the spectrum shown in the insertion. Both the formation and the initial decay of the signal are faster than the response time of the detection system. The exponential "tail" of these decay kinetics lasts into the tens of microseconds; at 60 K, a typical decay constant is $(1-3) \times 10^5$ s^{-1}. Judging from this time scale, the slow decay is due to spin−lattice relaxation in the radical in organic glasses.[18] By contrast, the fast component(s) seem to relate to the polarization dynamics in the radical−triplet complex.

4. Theory

Our results suggest that in a low-temperature glass, *p*-quinones form weakly bound molecular complexes with Tempo. This binding is weak; we do not find evidence for the molecular orbital perturbation in either moiety. Therefore, we believe that the magnetic parameters of the radical and the triplet are close to those of the matrix-isolated species (in that, we depart from the model suggested in refs 9 and 19). Two magnetic interactions between the triplet and radical moieties are considered: the spin exchange interaction and the electron dipole−dipole interaction. We assume that the former is isotropic and the latter can be treated in the point dipole approximation. All other magnetic interactions, as well as spin relaxation, are neglected. The latter assumption is reasonable, since in the low-temperature matrix, the time scale for the formation of the spin polarization is much shorter than the corresponding spin relaxation times.

We further assume that the excited doublet ($S = {}^1/_2$) states of the complex rapidly relax to yield a spin-polarized nitroxide radical bound to the ground S_0 state *p*-quinone; the relaxation of the quartet ($S = {}^3/_2$) states is much slower. We also assume that the interaction between the photoexcited quinone and the nitroxide radical is much weaker than the spin−orbit coupling in the *p*-quinone. Therefore, the intersystem crossing in the bound *p*-quinone molecule is assumed to occur in the same way as in an isolated *p*-quinone molecule. In such a case, the initial density matrix $\rho(t=0)$ of the radical−triplet complex by the time when the intersystem crossing is complete is given by the direct product of the density matrixes $\rho_T(t=0)$ of the triplet and $\rho_R(t=0)$ of the radical,

$$\rho(t=0) = \rho_R(t=0) \otimes \rho_T(t=0) = \frac{1}{N}\exp(-H_R/k_BT) \otimes \mathbf{T}\cdot\left(\frac{\mathbf{1}}{2} - \mathbf{P}\right)\cdot\mathbf{T} \quad (1)$$

where H_R is the spin Hamiltonian of the radical moiety, k_BT is the thermal energy, N is the normalization factor (so that $\mathrm{Tr}(\rho_{R-}) = 1$), and $\mathbf{T}$ is the spin of the triplet ($T = 1$). Tensor $\mathbf{P}$ in eq 1 has the same principlal axes *x*, *y*, and *z* as those of the dipole (ZFS) tensor of the *p*-quinone triplet; the corresponding principal values $p_i (i=x,y,z)$ are the initial populations of the triplet sublevels in the eigen basis $|\tau_i\rangle$ of the ZFS Hamiltonian, defined as $\mathbf{T}_i |\tau_i\rangle = 0$. [20] In the following, the principal axes of the **g** tensor of the nitroxide radical are used as a reference frame.

The spin Hamiltonian H of the radical−triplet complex is given by the sum of the contributions from the radical moiety (H_R), the triplet moiety (H_T), and the interaction term (H_{int}),

$$H_R = \mu_B \mathbf{B}_0 \cdot \mathbf{g}_R \cdot \mathbf{S} + \mathbf{S} \cdot \mathbf{A}_N \cdot \mathbf{I} \quad (2)$$

$$H_T = \mu_B g_T \mathbf{B}_0 \cdot \mathbf{T} + \mathbf{T} \cdot \mathbf{D}_T \cdot \mathbf{T} \quad (3)$$

$$H_{\{int\}} = -J_e\left(\frac{1}{2} + 2\mathbf{S}\cdot\mathbf{T}\right) + \mathbf{S}\cdot\mathbf{D}_{RT}\cdot\mathbf{T} \quad (4)$$

where μ_B is the Bohr magneton, $\mathbf{B}_0$ is the magnetic field of the spectrometer (whose orientation is given by the Euler angles Ω_B), $\mathbf{S}$ is the spin of the radical ($S = {}^1/_2$), $\mathbf{I}$ is the spin of the ^{14}N nucleus is the nitroxide radical ($I = 1$), $\mathbf{g}_R$ and $\mathbf{A}_N$ are the **g** tensor and the hyperfine coupling tensors for this radical, respectively, g_T is the isotropic *g* factor of the triplet, $\mathbf{D}_T$ is the ZFS tensor (whose principal axes are given by the Euler angles Ω_T), J_e is the spin exchange interaction, and $\mathbf{D}_{RT}$ is the point dipole tensor (whose principal axes are given by the Euler angles Ω_{RT}). We assume that the molecular complex possesses a well-defined geometry; that is, the Euler angles Ω_T and Ω_{RT} are fixed.

The time evolution of the density matrix $\rho(t)$ for the radical−triplet complex (whose initial state is given by eq 1) obeys the Liouville equation

$$\frac{d\rho}{dt} = i[\rho,H]_- - \frac{k_D}{2}[P_D,\rho]_+ - k_e\rho \quad (5)$$

where $P_D = {}^1/_4 - \mathbf{S}\cdot\mathbf{T}$ is the projector to the excited doublet states of the radical−triplet complex, k_D is the rate constant for the electronic system crossing of these doublet states to the ground state, and k_e is the rate constant for the spin-non-selective decay of a complex. The density matrix $\rho_R(t)$ of the radical (bound in the ground-state complex) can be found by integration of eq 5 and taking the trace over the triplet states:

$$\rho_R = \int_0^t d\tau Tr_T\{k_D P_D \rho(\tau) P_D + k_e\rho(\tau)\} \quad (6)$$

For a given orientation Ω_B of the magnetic field, the excess spin polarization $P_R(\Omega_B;t)$ in the radical is given by the expectation value for the projection of the radical spin on the unit vector $\mathbf{u} = \mathbf{g}_R\mathbf{u}_B/g_R$, where $g_R^2 = \mathbf{u}_B\mathbf{g}_R\mathbf{u}_B$ and $\mathbf{u}_B$ is the unit vector in the direction of the magnetic $\mathbf{B}_0$ field

$$P_R(\Omega_B;t) = 2\,Tr_R(\mathbf{S}\cdot\mathbf{u}\rho_R(t)) - P_{eq} \quad (7)$$

where the trace is taken over the spin states of the radical and $P_{eq} = \tanh(\hbar\omega/2k_BT)$ is the thermal polarization.

The calculation proceeds in the following way. First, for a given orientation Ω_B and the microwave frequency ω, resonance fields B_0 for the radical in the ground-state molecular complex are calculated using the standard first-order perturbation theory,[21] in which $H_R \approx \omega\ \mathbf{S}\cdot\mathbf{u}$ and $\rho(t=0) \approx \{1\}/\{2\} - P_{eq}\mathbf{S}\cdot\mathbf{u}$. Then, eq 5 is solved numerically, using the singular value decomposition algorithm. The polarizations $P_R(\Omega_B;t)$ are calculated using eqs 6 and 7 and plotted against the corresponding resonance fields B_0. The histogram for 5×10^3 randomly sampled orientations Ω_B is convoluted with a Gaussian line width function (0.5 mT fwhm). This procedure yields a "powder" TR EPR spectrum of the ground-state molecular complex. Alternatively, the polarization $P_R(\Omega_B;t)$ is integrated over *all* orientations Ω_B of the molecular complex to give the total radical polarization $P_R(t)$.

To implement this model, many parameters must be known: the initial triplet populations, ZFS and point dipole tensors, the exchange interaction J_e, and the rate constants k_D and k_e. None of these parameters are known with certainty (see below). On the other hand, we do not intend to simulate the data. Rather,

we are interested whether the general trends observed in our experiments can be reproduced using this model. In particular, we want to know what is the most important mechanism for the spin polarization in the radical−triplet complex? Is the spin polarization transferred to the radical from the triplet (as assumed in the ESPT mechanism)? Or is it developed due to the effects of exchange on the spin sorting in the radical−triplet complex (as assumed in the RPTM)? As mentioned in the Introduction, no specific ESPT mechanisms have been discussed in the past. Apparently, most researchers believe that the spin sorting has little effect on the ESPT: the transfer is solely due to the spin exchange. This does not seem reasonable: if the spin sorting occurs in the encounters of free radicals with *thermalized* triplets, then it also occurs in the encounters of these radicals with *spin-polarized* triplets. If the spin-selective electronic relaxation causes significant polarization in the former type of encounters, why would that be different for the latter type of encounters?

For the molecular complexes in glasses, this question may be settled using the model given above. For example, one can follow the spin polarization for a complex in which the triplet is initially polarized, and let $k_D = 0$ (no spin selection): this would correspond to ESPT. Alternatively, one can start with a thermalized triplet and let $k_D \neq 0$: this would correspond to RTPM. We may further idealize the system, by letting $H_{int} = 0$, and disentangle the effects of the spin exchange and the spin-selective reaction. In the end, we would determine what contribution, in what parameter range, has most effect on the resulting spin polarization (section 5.2).

The principal difficulty in the realization of this program is that most parameters used in the simulations are not known. Some of these parameters may be estimated using the data in the literature (section 5.1), others guessed. Fortunately, some trends may be studied under very general assumptions, by careful examination of the equations of motion using the tensor operator formalism. Given the technical complexity of this approach, this examination is placed in the Supporting Information. The results obtained therein are taken for granted in the rest of the manuscript.

Below, we argue that neither ESPT alone nor RTPM alone (in the narrow sense used above) are sufficient to explain the data. Apparently, these two mechanisms work in concert.

5. Discussion

5.1. Model Parameters. Following the previous section, we assume that the orbital perturbation of the triplet state by the nitroxide radical is negligible. The UV excitation of 1,4-benzoquinone yields two $^3n\pi^*$ states with the D_{2h} symmetry, ^3A_u, and $^3B_{1g}$. The electronic energy of these triplet states is 18 500 cm^{-1} (relative to the ground S_0 state) and the gap between these two states is 300 cm^{-1}.[22] Due to the quasi-degeneracy of the triplet terms, the vibronic coupling between these states is strong, and the lowest B_{1g} term contains a double minimum potential.[23] As a result, the lowest triplet level is further split into the zero-point (*g*-inversion) level and the vibronic (*u*-inversion) level: the splitting between these two levels is ca. 20 cm^{-1}.[23] For 1,4-benzoquinone-h_4 in 1,4-benzoquinone-d_4 host crystals, the ZFS parameters for these two levels are different: for the lower *g*-inversion state, $D = -0.07$ cm^{-1}; for the higher *u*-inversion state, $|D| = 0.33$ cm^{-1}.[23] For the latter state, both the sign of D and the orientation of the principal axes of the ZFS tensor in the molecular frame are not known. TR EPR spectra from the excited triplet states of the 1,4-benzoquinone, 1,4-naphthoquinone, and 9,10-anthraquinone in low-temperature organic glasses[24] are consistent with $|D| = 0.33$ cm^{-1}. This suggests that the triplet quinones are in the *u*-inversion state. Consequently, the dipole tensor of these triplets is not known. From general considerations, we assume that $D = -0.33$ cm^{-1} (−10 GHz), $p_x \approx p_y$, and the long axis Z of the ZFS tensor is along the carbonyl bond (in agreement with Murai et al.). [24] We also assume that the **g** tensor of the triplet is isotropic, with $g_T = 2.005$. Murai et al. [24] estimated that in organic glasses, the initial populations of the triplet states for the 1,4-benzoquinone, 1,4-naphthaquinone, and 9,10-anthraquinone (for the ZFS tensor orientation given above) are $p_z = 0.8$ and $p_x = p_y = 0.1$.

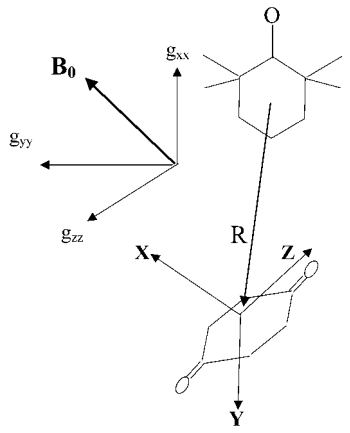

Figure 5. The coordinate frames used in the theoretical model. The coordinate frame of the principal axes of radical **g** tensor is used as the reference frame. The *z* axis of the **g** tensor points in the direction of the N 2p orbital in the SOMO.

The **g** and hyperfine coupling (**A**[^{14}N]) tensors of Tempo are coaxial. [25] In low-temperature toluene glass,[25,26] the principal values are $g_{xx} = 2.0098$, g_{yy}=2.0062, and $g_{zz} = 2.0022$, and $A_{xx} = 0.6$ mT, $A_{yy} = 0.7$ mT, and $A_{zz} = 3.45$ mT (the principal axes are shown in Figure 5).

From our simulations, it appears that for realistic intermolecular distances (>0.65 nm) and spin exchange constants $|J_e|$ (>10 GHz), the dipolar intermolecular interaction in eq 4 may be neglected.

The rate constant k_D cannot be faster than the rate constant of the intersystem crossing in the *p*-quinone. For aqueous 1,4-benzoquinone, the S_1-T_1 crossing occurs in 20 ps.[27] Watkins[28] and Scaiano[1] have found that the quenching rate of the T_1 states of aromatic hydrocarbons by nitroxide radicals is diffusion controlled for the triplets whose energy exceeds ca. 20000 cm^{-1}. For 1,4-benzoquinone and 9,10-anthraquinone in organic solutions, these triplet energies are 18 700 and 21 800 cm^{-1}. That is, the quenching is diffusion controlled. Given that there is a pronounced RTPM polarization in the *p*-quinone/Tempo solutions at 298 K, we estimate that k_D is 10^8-10^9 s^{-1} (which is close to the inverse lifetime of the encounter complex in these room-temperature solutions). The rate constant k_e should be close to the inverse lifetime of the *p*-quinone triplet. In the low-temperature glass, these times are $10^{-5}-10^{-4}$ s.

5.2. Simulations. Figure 6b, traces i and ii, show TR EPR spectra calculated at the delay time $t = 5$ μs for two orientations of the $\mathbf{D}_T$ tensor (see the caption to Figure 6 and the diagram in Figure 5) and the following model parameters: $J_e = -14$ GHz (−0.47 cm^{-1}), $k_e = 4 \times 10^5$ s^{-1}, $k_d = 10^8$ s^{-1}, $D = -0.33$ cm^{-1}, $E = 0.02$ cm^{-1}, and $p_z = 0.8$ ($p_x = p_y = 0.1$). In Figure 6a, normalized TR EPR spectrum shown in Figure 6b, trace ii, is compared to a simulated EPR spectrum of the thermalized nitroxide radical. For these model parameters, the resulting TR

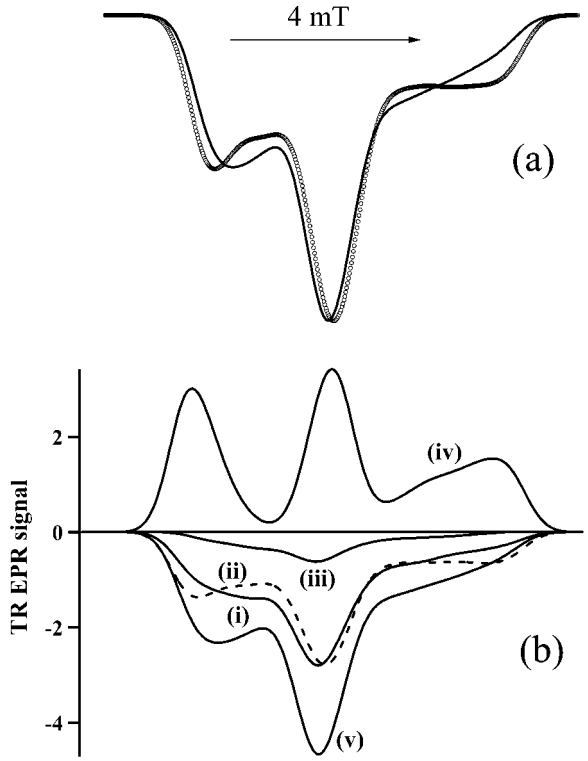

Figure 6. Simulated TR EPR spectra obtained using the theoretical model of section 4, for $t = 5$ μs, $D = -0.33$ cm^{-1}, and $E = 0.02$ cm^{-1}. (a) A comparison between the line shapes of the normalized TR EPR spectrum shown separately in Figure 6b, trace ii, (open circles) and the normalized EPR spectrum of a thermalized nitroxide radical (solid line). In traces b, the polarization is given in units of thermal polarization at 60 K. The following parameters were used for traces (i) and (ii): $J_e = -14$ GHz, $k_e = 4 \times 10^5$ s^{-1}, $k_D = 10^8$ s^{-1}, $p_x = p_y = 0.1$, $p_z = 0.8$, and $\Omega_T = (0°, 90°, 0°)$ (trace i) and $\Omega_T = 0$ (trace ii). All other EPR spectra were calculated for $\Omega_T = 0$. Trace iii was obtained for the same model parameters as trace (i) except for the initial triplet population, $p_x = p_y = p_z = 1/3$, and $k_e = 4 \times 10^6$ s^{-1}. Trace (iv) was calculated for the same model parameters as trace i, except for $k_e = 0$ and $J_e = 0$. Trace v was calculated for $J_e = -14$ GHz, $p_x = p_y = 0.1$, $p_z = 0.8$, $k_e = 4 \times 10^5$ s^{-1}, and $k_D = 0$.

EPR spectra relatively weakly depend on the orientation of the triplet (e.g., compare traces i and ii). Typical absolute spin polarizations obtained in these simulations are 3−4 times the thermal polarization at 60 K, which is ca. 0.02 in the X band.

In general, for $|J_e| < |D|$, the sign of the polarization can be positive or negative depending on the delay time t, the kinetic parameters k_D and k_e, and the orientation of the triplet. The experimental TR EPR spectra from Tempo are emissive, for all photosystems, and for all delay times. One may expect that the exchange interaction J_e and the initial triplet polarization vary between these photosystems. However, if this exchange is always large, so that $|J_e| > |D|$, the line shapes of the resulting EPR spectra will all be similar. If the latter condition is fulfilled, the phase of the TR EPR spectrum is given by sign of the exchange constant J_e; this phase does not depend on $|J_e|$, the kinetic parameters, the delay time t, etc. Note that in this regime, the intensity of the TR EPR signal decreases as the exchange constant increases.

Figure 6b, trace iii, demonstrates a TR EPR spectrum calculated for $t = 5$ μs, $p_x = p_y = p_z = 1/3$ (no initial triplet polarization), $k_e = 4 \times 10^6$ s^{-1}, $k_D = 10^8$ s^{-1}, and $J_e = -14$ GHz. Such a situation corresponds to "pure" RTPM (in the narrow sense given in section 4). The EPR signal is relatively small; the absolute polarization is comparable to that of a thermalized radical. Depending on the rate constant k_D, the delay time t, and the orientation Ω_T of the triplet, one can obtain almost any kind of EPR spectrum, including the absorptive spectrum similar to the one shown in Figure 6b, trace iv. Thus, "pure" RTPM is overly sensitive to the model parameters. We conclude that to obtain realistic EPR spectra, considerable initial spin polarization in the triplet *p*-quinone is needed; otherwise, the TR EPR spectra would be qualitatively different for different photosystems.

For comparison, Figure 6b, trace iv, shows the EPR spectrum obtained for the same parameters as Figure 6b, trace ii, save for $J_e = 0$ and $k_e = 0$. The mechanism for the formation of spin polarization for $J_e \approx 0$ is discussed in section 1S. For $k_D/D \ll 1$, the spin polarization is weak: it becomes stronger when the triplet is initially polarized, see Figure 6b, trace iv. However, both the line shape and the phase of this spectrum are different from the experimental EPR spectra shown in Figures 1−3. For $J_e = 0$, the completely emissive EPR spectra at $t = 0.1-1$ μs can be obtained only for $k_D > 10^{11}$ s^{-1}: that would be unrealistically fast. Apparently, a spin sorting reaction alone cannot account for the experimental observations.

Figure 6, trace v, shows the calculated TR EPR spectrum for "pure" ESPT (in the narrow sense given in section 4), obtained for $J_e = -14$ GHz, $k_e = 4 \times 10^5$ s^{-1}, and $k_D = 0$. This EPR spectrum is emissive, as may be anticipated from the analytical results of section 1S. The EPR line shape is similar (although not exactly the same) as that for the thermalized nitroxide radical. Note that "pure" ESPT yields is the greatest negative signal among the EPR spectra shown in Figure 6(b).

The simulations with $p_z \sim 1$, $|J_e/D| \sim 1-5$, and $k_D \sim 10^8-10^9$ s^{-1} consistently yield TR EPR spectra whose line shapes just slightly deviate from the EPR spectra of the thermalized radical (Figure 6a). These deviations may be traced to the polarization that is formed or transferred due to spin-selective reaction in the radical−triplet complex. As mentioned in section 3, all TR EPR spectra obtained shortly after the photoexcitation event exhibit such deviations, albeit to a different degree. While the small-scale deviations similar to those shown in Figure 6a naturally emerge in our simulations, for no model parameters did we obtain the spectra similar to those shown in Figure 3a.

The observed polarization kinetics also point to the occurrence of the spin-selective reaction. To demonstrate that, consider a special case of a molecular complex whose $\mathbf{g}_R$ and $\mathbf{D}_T$ tensors are coaxial, the triplet *p*-quinone is initially populated in the T_x state ($p_x = 1$), and the magnetic field $\mathbf{B}_0$ directed along axis y of the radical $\mathbf{g}$ tensor (Figure 5).

Figure 7, trace i, exhibits the kinetics obtained for "pure" ESPT in such a model complex ($k_e = 6 \times 10^5$ s^{-1}, $k_D = 0$, and $J_e = -14$ GHz). The time-dependent total polarization monotonically approaches a negative asymptotic value with rate constant k_e. The spin polarization does not change for $t > k_e^{-1}$, because the spin relaxation in the radical is neglected. Since in our system $k_e \sim 10^4-10^5$ s^{-1}, the formation time for the polarization due to "pure" ESPT should be on the time scale of tens of microseconds. Experimentally, the formation time is shorter than the response time of our detection system (ca. 200 ns). A rapid spin-sorting reaction is needed to speed up the polarization transfer (section 1S).

Figure 7, trace iv, shows the polarization kinetics obtained for $k_D = 10^8$ s^{-1}, $k_e = 0$, and $J_e = -14$ GHz. It is seen that the formation time of the emissive polarization is ca. 1 μs; this polarization fully decays in 20 μs. For $k_e = 0$, the polarization asymptotically approaches zero for orientations in which the magnetic field $\mathbf{B}_0$ is directed along the principal axes of the

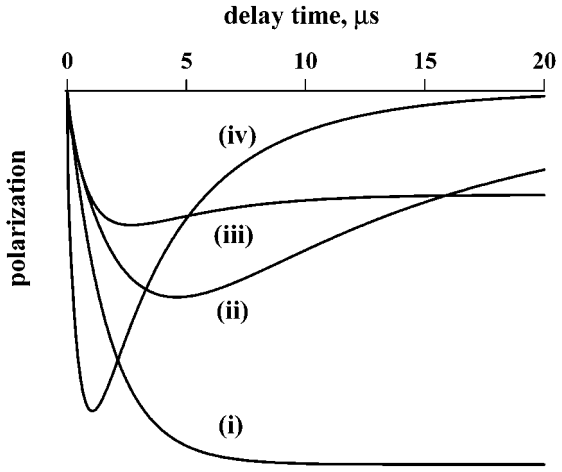

Figure 7. The kinetics of spin polarization for a model complex with coaxial $\mathbf{D}_T$ and $\mathbf{g}_R$ tensors. In traces i and iv, the magnetic field $\mathbf{B}_0$ is oriented along axis *y* of the radical **g** tensor. In traces ii and iii, $\mathbf{B}_0$ lays in the *xy* plane making an angle of 45° with the *x* and *y* axes. All traces were obtained for $D = -0.33$ cm^{-1}, $E = 0.02$ cm^{-1}, and $p_x = 1$. Trace (i) is obtained for $J_e = -14$ GHz, $k_e = 6 \times 10^5$ s^{-1}, and $k_D = 0$. Traces ii−iv are obtained for $k_e = 0$, $k_D = 10^8$ s^{-1}, and $J_e = -14$ GHz (traces iii and iv) or $J_e = -25$ GHz (trace ii).

radical g-tensor, regardless of the initial triplet polarization (Figure 7, trace iv). For an arbitrary orientation of the molecular complex relative to the magnetic field, the polarization decays to a negative asymptotic value that depends on the model parameters (Figure 7, trace iii). An increase in $|J_e|$ slows down both the formation and decay kinetics of the spin polarization, as illustrated in Figure 7, traces iii and ii (−25 vs −14 GHz). From the dependence of the kinetics on the exchange constant, a rough upper bound limit for J_e can be obtained: $|J_e/D| < 5$. The introduction of a slow nonselective decay ($k_e < 10^6$ s^{-1}) leads to the kinetics similar to those shown in Figure 7, trace ii). Note that, for $k_e p = 0$, the polarization always reaches a negative asymptotic value. If one convolutes the polarization kinetics shown in Figure 7, trace iii, with an exponential decay due to spin−lattice relaxation in the radical, one obtains the bimodal kinetics shown in Figure 4.

While our model qualitatively accounts for the EPR spectra and the polarization kinetics, it cannot yield the correct estimate for the formation time of the spin polarization for $|J_e| > |D|$. For $k_D < 10^9$ s^{-1}, the formation times of 0.1−0.3 μs may be obtained only for $|J_e| < 1$ GHz. As explained above, for such small exchange constants, the shape of EPR spectrum is too sensitive to the model parameters. It is presently unclear, whether this discrepancy indicates that our model is incomplete or that the estimates for the spin parameters (such as *D*) are incorrect. More work is needed to resolve this conundrum.

Our insistence on the pivotal role of rapid spin selective depopulation of the photoexcitied molecular complex is mainly due to the difficulty of finding a sufficiently fast spin-independent decay reaction that occurs at 20−60 K. In principle, it is possible to find the model parameters for which "pure" ESPT alone can account both for the TR EPR spectra and their time evolution. In our judgment, these model parameters are unrealistic. On the other hand, our theoretical model disregards spin relaxation in the radical−triplet complex. If there were a rapid spin relaxation in the triplet manifold of this complex, it could have accounted for the fast formation kinetics. However, in such a case, the nitroxide radical would be bound to a spin relaxed T_1 state rather than the ground S_0 state of the *p*-quinone. As there is a strong spin exchange interaction between the radical and the triplet moieties, the EPR spectrum of such a complex would be different from that of the isolated nitroxide radical. In the model examined in section 4, the EPR signal from the radical−triplet complex is neglected: only ground-state molecular complexes are assumed to contribute to the observed EPR signal from Tempo. Therefore, a contribution from the radical−triplet complexes that involve a magnetically relaxed triplet *p*-quinone is neglected. This may be the crucial deficiency of our model.

6. Concluding Remarks

The formation of electron spin polarization in a nitroxide radical bound to a *p*-quinone in a molecular complex in low-temperature organic glass is demonstrated. The photoexcited *p*-quinone/radical complex undergoes rapid intersystem crossing to yield a matrix-isolated radical−triplet pair; this pair decays mainly due to the electronic relaxation of excited doublet states of this complex. The spin polarization in the radical moiety of the matrix-isolated complex is formed in less than 300 ns and decays on the time scale of tens of microseconds No degradation of the TR EPR signal from the polarized nitroxide radical after $>10^4$ laser excitation cycles is observed. Large polarization yield and remarkable photostability make these complexes an attractive choice for several practical applications, such as microwave amplification[29] and quantum computing (see the Introduction).[13−17]

A theoretical model for the formation of spin polarization in the matrix-isolated radical−triplet pairs is suggested. This model is conceptually similar to the models that were previously suggested for RTPM in liquid solutions. Due to the simplification of molecular dynamics in the rigid environment, we were able to concentrate on the peculiarities of *spin dynamics* in such radical−triplet pairs. No such possibility exists for the radical−triplet pairs in liquid solutions, because their spin dynamics are strongly influenced by the encounter dynamics and spin relaxation in the triplet. For the matrix-isolated radical−triplet pairs, we demonstrate that several polarization mechanisms operate *in concert* to produce the observed polarization dynamics. In particular, three such mechanisms have been recognized:

In ESPT, the initial polarization in the triplet moiety is transferred to the radical due to electron spin exchange and electron dipole−dipole interaction between the triplet and the radical moieties. No spin-selective relaxation of the excited states is needed to produce the spin polarization. In the photosystems studied in the present work, this mechanism provides the greatest contribution to the spin polarization in the nitroxide radical.

Another mechanism, that we name QIPM (for quenching-induced polarization mechanism) operates without any magnetic interaction between the triplet and radical moieties. In QIPM, the spin polarization is formed exclusively due to the occurrence of rapid depopulation of the doublet states of the radical−triplet complex; no initial spin polarization in the triplet is needed. When this initial triplet polarization is present, QIPM efficiently "transfers" it to the radical moiety, in a different manner than ESPM (see section 1S). As a result, the polarization "transferred" by QIPM may be different or even opposite in sign to that transferred by ESPT. In the *p*-quinone/Tempo complexes, this "transfer" considerably speeds up the formation of the spin polarization in Tempo.

In RTPM, the spin-selective reaction and the exchange interaction act in concert. As in QIPM, no initial spin polarization in the triplet is needed. Formally, QIPM is a special case of RTPM. The distinction between these two mechanisms is a matter of convenience: one examines which player, the spin exchange or the spin sorting, has a greater effect on the resulting

spin polarization and its kinetics. Our simulations indicate that for realistic rate constants k_D of the spin-selective relaxation of the radical−triplet complex (10^8-10^9 s^{-1}) and realistic spin exchange constants J_e ($|J_e/D| < 5$), the spin exchange interaction is far less important than the spin-selective reaction. Essentially, it is QIPM rather than RTPM that yields the polarization in the nitroxide radical. The initial triplet polarization is transferred to the radical moiety by ESPT and QIPM acting together, in concert.

In practice, these three mechanisms are not additive and cannot always be separated, being formulated in terms of the same master Liouville eq 5. However, in some cases, it may be possible to determine which one of these three idealized mechanisms is responsible for the observed polarization patterns, as the resulting TR EPR signals differ in their phase, kinetics, magnitude, and (in a solid) even the line shape of the spectrum. Perhaps, as the studies of the chemically bound radical−triplet pairs progress further, there will be more examples of specific action of these three distinct mechanisms.

Supporting Information Available: 1S. Appendix: Tensor operator formalism for modeling spin dynamics in radical−triplet pairs. This material is available free of charge via the Internet at http://pubs.acs.org.

References and Notes

(1) Scaiano, J. C. *Chem. Phys. Lett*. **1981**, *79*, 441. Kuzmin, V. A.; Tatikolov A. S.; Borisevich, Yu. E. *Chem. Phys. Lett*. **1978**, 53, 52. Schwerzel, R. E.; Caldwell, R. A. *J. Am. Chem. Soc*. **1973**, *95*, 1382.

(2) Thurnauer, M. C.; Meisel, D. *Chem. Phys. Lett*. **1982**, *92*, 343.

(3) Imamura, T.; Onitsuka, O.; Obi, K. *J. Phys. Chem*. **1986**, *90*, 6741.

(4) Blättler, C.; Paul, H. *Chem. Phys. Lett*. **1990,** *166*, 375. Tarasov, V. V., Ph.D. Thesis, University of Zürich, Zürich, Switzerland, 1999.

(5) Blank, A.; Levanon, H. *J. Phys. Chem*. A **2000**, *104*, 794.

(6) Shushin, A. I. *Chem. Phys. Lett.* **1999**, 313, 246; *Chem. Phys. Lett*. **1993**, *208*, 173; *J. Chem. Phys*. **1993**, *99*, 8723.

(7) Adrian, F. J. *Chem. Phys. Lett.* **1994**, *229*, 465.

(8) Kobori, Y.; Takeda, K.; Tsuji, K.; Kawai, A.; Obi, K. *J. Phys. Chem.* A **1998**, *102*, 5160.

(9) Ishii, K.; Hirose, Y.; Fujitsuka, H.; Ito, O.; Kobayashi, N.; *J. Am. Chem. Soc*. **2001**, *123*, 702.

(10) Fujisawa, J.; Ishii, K.; Ohba, Y.; Yamauchi, S.; Fuhs, M.; Möbius, K. *J. Phys. Chem.* A **1999**, *103*, 213.

(11) Mizuochi, N.; Ohba, Y.; Yamauchi, S. *J. Phys. Chem.* A **1999**, *103*, 7749; Corvaja, C.; Maggini, M.; Ruzzi, M.; Scorrano, G.; Toffoletti, A. *Appl. Magn. Reson*. **1997**, *12*, 477.

(12) Corvaja, C.; Franko, L.; Toffoletti, A. *Appl. Magn. Reson*. **1994**, *7*, 257.

(13) Knight, P. *Science* **2000**, *287*, 441; DiVincenzo, D. P. *J. Appl. Phys*. **1997**, *81*, 4602; Bennett, C. H.; DiVinchenzo, D. P. *Nature* **2000**, *404*, 247. Grushka, J. *Quantum Computing*; McGraw-Hill: London, 199.

(14) Prinz, G. A. *Science* **1998**, *282*, 1660, *J. Magn. Magn. Mater.* **1999**, *200*, 57. Das Sarma, S.; Fabian, J.; Hu, J.; Zutic, I. *Superlattices Microstruct.* **2000**, *27*, 289.

(15) Gershenfeld, N. A.; Chuang, I. L. *Science* **1997**, *275*, 350; Chuang, I. L.; Vandersypen, L. m. K.; Zhou, X.; Leung, D. W.; Lloyd, S. *Nature* **1998**, *393*, 143. Somaroo, S.; Tseng, C. H.; Havel, T. F.; Laflamme, R.; Cory, D. G. *Phys. Rev. Lett.* **1999**, *82*, 5381.

(16) Kane, B. E. *Nature* **1998**, *393*, 133.

(17) Burkard, G.; Loss, D.; DiVincenzo, D. P. *Phys. Rev. B* **1999**, *59*, 2070.

(18) Dzuba, S. A.; Tsvetkov, Yu. D. *Chem. Phys.* **1988**, *120*, 291.

(19) Chiu, Y.-N. *J. Chem. Phys*. **1972**, *56*, 4882.

(20) Atkins, P. W.; Evans, G. T. *Mol. Phys*. **1974**, *27*, 1633.

(21) Thuomas, K.-Å.; Lund, A. *J. Magn. Res.* **1975**, *18*, 12.

(22) Trommsdorff, H. P. *J. Chem. Phys*. **1972**, *56*, 5538

(23) Lichtenbelt, J. H.; Fremeyer, J. G. F. M.; Veenvliet, H.; Wiersma, D. A. *Chem. Phys*. **1975**, *10*, 107. Veenvliet H.; Wiersma, D. A. *J. Chem. Phys*. **1974**, *60*, 704.

(24) Murai, H.; Minami, M.; Hayashi, T.; I'Haya, Y. J. *Chem. Phys*. **1985**, *93*, 333.

(25) Hwang, J. S.; Mason, R. P.; Hwang, L.-P.; Freed, J. H. *J. Phys. Chem*. **1975**, *79*, 489.

(26) Grinberg, O. Ya.; Dubinskii, A. A.; Shestakov, A. P.; Lebedev, Ya. S. *Khim. Phizika* **1983**, *1*, 54 (in Russian).

(27) Rossetti, R.; Brus, L. E. *J. Am. Chem. Soc.* **1986**, *108*, 4718.

(28) Watkins, A. R. *Chem. Phys. Lett*. **1974**, *29*, 526. *Chem. Phys. Lett*. **1980**, *70*, 262.

(29) Blank, A.; Levanon, H. *Appl. Phys. Lett.* **2001**, *79*, 1694.